Sciencexpress Reports

Robust Photogeneration of H_2 in Water Using Semiconductor Nanocrystals and a Nickel Catalyst

Zhiji Han,* Fen Qiu,* Richard Eisenberg,† Patrick L. Holland,† Todd D. Krauss†

Department of Chemistry, University of Rochester, Rochester, NY 14627, USA.

*These authors contributed equally to this work.

†To whom correspondence should be addressed. E-mail: eisenberg@chem.rochester.edu (R.E.); holland@chem.rochester.edu (P.L.H.); krauss@chem.rochester.edu (T.D.K.)

Homogeneous systems for light-driven reduction of protons to H_2 typically suffer from short lifetimes because of decomposition of the light-absorbing molecule. We report a robust and highly active system for solar hydrogen generation in water that uses CdSe nanocrystals capped with dihydrolipoic acid (DHLA) as the light absorber and a soluble Ni^{2+}-DHLA catalyst for proton reduction with ascorbic acid as an electron donor at pH 4.5, which gives > 600,000 turnovers. Under appropriate conditions, the precious-metal-free system has undiminished activity for at least 360 hours under illumination at 520 nm, and achieves quantum yields in water of over 36%.

Molecular hydrogen (H_2) is a clean-burning fuel that can be produced from protons (H^+) in the reductive half-reaction of artificial photosynthesis systems (*1*, *2*). One of the most prominent strategies for light-driven proton reduction features a multicomponent solution with a light absorbing molecule (chromophore) that transfers electrons to a catalyst that reduces protons (*3*, *4*). However, these solution systems often use nonaqueous solvents, and always have short lifetimes from decomposition of the chromophore over a period of hours (*5*). This difficulty has led to more complicated architectures that separate the sites of light absorption and proton reduction (*2*).

Semiconductor nanocrystals (NCs) are promising alternative chromophores for light driven proton reduction (*6*, *7*). Compared to traditional organic or organometallic chromophores, NCs have superior photostability, larger absorption cross-sections over a broad spectral range, orders of magnitude longer excited state lifetimes, electronic states and associated optical properties that vary with NC size, and the capacity to deliver multiple electrons with minimal structural perturbations (*6*, *7*). Heterostructures combining NCs with traditional precious metal nanoparticle proton reduction catalysts, or with iron-hydrogenases, have produced efficient proton reduction catalysis in solution (*8*–*10*). However, small-molecule catalysts in conjunction with NCs have given only modest H_2 production (*11*, *12*).

We report here a system that provides light-driven H_2 production with exceptional longevity, maintaining its high activity with no decrease for over two weeks using water as solvent. The system uses no precious metals, and is based on light absorption and photoinduced electron transfer from semiconductor nanocrystals that are photochemically stable. Under optimal conditions, the system generates over 600,000 turnovers of H_2 (with respect to catalyst) without deterioration of activity, and thus has significant promise for incorporation into full artificial photosynthesis (AP) systems.

Hydrophobic CdSe NCs with diameters varying from 2.5 to 5.5 nm (defined based on the wavelength of the peak in their lowest energy excitonic absorption feature as NC(520) and NC(620) respectively, Fig. S1) were synthesized by variations of literature methods (*13*, *14*). These NCs were subsequently rendered water soluble by capping with dihydrolipoic acid (DHLA, Fig. 1) (14). Photochemical experiments were performed in a custom-built 16-sample apparatus with excitation at 520 nm and a measurement uncertainty of 7.0% in the amount of H_2 produced (based on multiple-run experiments). Each 40 mL sample vessel contained 5.0 mL of solution, a cap with a sensor to allow real-time monitoring of head space pressure, and a port for quantitative analysis of H_2 production.

In a complete artificial photosynthesis system, two molecules of water are photochemically split into H_2 (reductive side) and O_2 (oxidative side) (*1*, *2*). Electrons from the oxidative side of the system are shuttled to the reductive side where they reduce protons to hydrogen. However, due to the complexity in building and optimizing such a complete artificial photosynthesis system, when studying the reductive half-reaction it is common for a sacrificial electron donor to be used to optimize catalysts for hydrogen production. Here, ascorbic acid (AA, 0.1 to 1.0 M) was used as the sacrificial electron donor, because reduction of protons by ascorbate is thermodynamically unfavorable ($\Delta E = -0.41$ V) under these conditions (*15*), and light energy is needed to bring about H_2 production (Fig. 1). Thus it provides "proof of principle" regarding photochemical proton reduction.

In a typical experiment, production of hydrogen occurred upon irra-

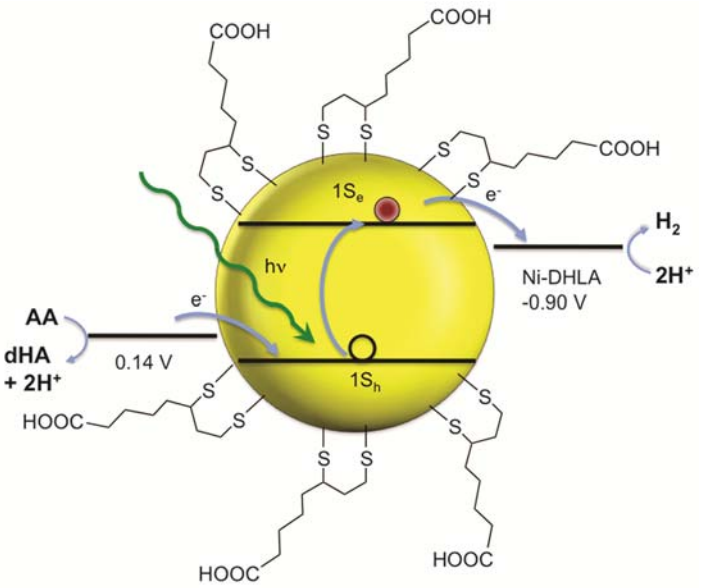

Fig. 1. Cartoon that illustrates the relevant energies for H_2 production (Abbreviations: AA, ascorbic acid; dHA, dehydroascorbic acid). Potentials are shown vs normal hydrogen electrode (NHE) at pH = 4.5.

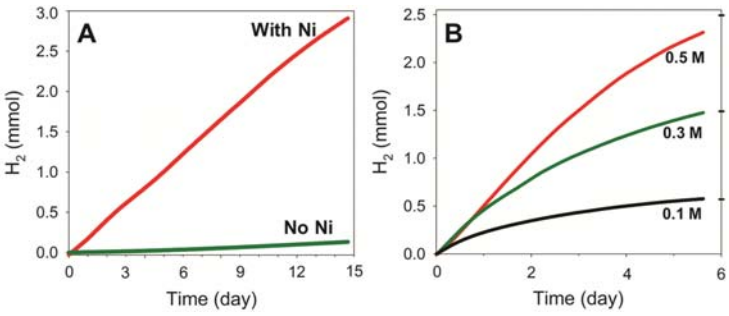

Fig. 2. (A) H_2 production over time from irradiation of an aqueous solution of [$Ni(NO_3)_2$], NC(540), and AA **(B)** Photoreductive H_2 production with different initial concentrations of AA in a system containing 20.0 μM [$Ni(NO_3)_2$] and 1.0 μM [NC(570)]. The marks on the right axis indicate the theoretical maximum of H_2 production based on the amount of AA added. Hydrogen photogeneration experiments used a light-emitting diode (LED) source (λ = 520 nm, 13 mW cm^{-2}) at 15°C and 1 atm initial pressure of N_2:CH_4 (79:21 mol %) with CH_4 as an internal standard for H_2 quantification by GC analysis.

diation (λ = 520 nm) of a solution formed from nickel(II) nitrate and NCs in water. Under appropriate conditions (10.0 μM [$Ni(NO_3)_2$], 0.5 μM [NC(570)], and 1.0 M AA) the system continues to produce H_2 at a constant rate for over 360 hours (Fig. 2A). A control experiment without added Ni^{2+} yielded no significant H_2 production (Fig. 2A). The unusual longevity is attributed to the use of NCs as the photosensitizer, because other systems using transition metal catalysis and small-molecule photosensitizers (organic dyes, or Ru, Ir, Rh or Re coordination compounds) cease activity in under 50 hours due to bleaching of the dye (*16–22*). Other recent reports have described NC photosensitizers in systems for H_2 production, but the activity and longevity were not comparable to those described here (*11*, *12*).

Using different concentrations of system components that were chosen to maximize catalyst activity (1.0 μM [$Ni(NO_3)_2$], 5.0 μM [NC(540)], and 0.8 M AA, pH 4.5 in water), this same system achieves a turnover number (TON) over 600,000 mol H_2/mole catalyst after 110 hours and an initial turnover frequency (TOF) of 7,000 mol H_2/mole catalyst/hour upon irradiation with 520 nm light (Fig. S2). The slight decrease in H_2 production rate in Fig. S2 results from depletion of AA as the electron donor and not from photochemical instability, as evidenced by the increasing lifetime of H_2 production with higher starting concentrations of AA (Fig. 2B). Even higher activity is obtained under the same irradiation conditions if the solvent is changed to 1:1 EtOH/H_2O (Fig. S3). The initial rate of H_2 production is saturated above [AA] = 0.3 M (Fig. 2B), and slows over time only upon depletion of the electron donor AA. Consistent with this interpretation, subsequent addition of AA restarts H_2 production (Fig. S4).

We hypothesize that the catalytic system functions through light absorption by the CdSe nanocrystal, electron transfer to the catalyst, and then proton reduction by the catalyst. The oxidation of AA, which fills the photogenerated hole on the NC, leads to dehydroascorbic acid + 2 e^- + 2 H^+. Ascorbic acid thus serves as both a potential source of hydrogen and as a buffer due to the production of the conjugate base, helping to maintain the acidic pH even as protons are reduced to hydrogen. The absorption of the first excitonic state can be controlled by NC size, which correlates with the reduction potential of the excited state (*23*). In our photocatalytic H_2 production system, reducing NC size leads to an increase in the activity (Fig. 3A), which we attribute to an increase in NC reducing power. Conversely, there is no formation of H_2 with NC(620), presumably because the reduction potential for NC(620) lies below that needed for catalyst activity (*12*). Because the NC absorption edge is to the blue of the LED spectral emission profile, the system with NC(520) produces less H_2 than an identical one with NC(540).

Organic electron acceptors were also used as indicators for the reducing power of the CdSe NCs. When a 3.8 μM solution of NC(530) in 1:1 EtOH/H_2O was irradiated in the presence of methyl viologen dication (MV^{2+}) under N_2 for 5 min, a color change from orange to blue indicated formation of reduced viologen $MV^{+\bullet}$. A similar result was obtained using a diquat acceptor DQ^{2+} (*N*,*N*′-(1,3-propylene)-5,5′-dimethylbipyridine), as indicated by the pink color of the reduced $DQ^{+\bullet}$ (Fig. S5). Although the precise potential for each NC was not determined, the result for DQ^{2+} suggests that the reducing ability of NC(530) corresponds to a potential more negative than -0.7 V vs. NHE, and thus the excited state is sufficiently reducing for H^+ reduction. These measurements agree with published cyclic voltammetric studies that indicate a reduction potential more negative than -1 V for CdSe NCs of this size (*23*).

The catalytic mechanism was evaluated by varying the concentrations of system components. When [Ni^{2+}] was varied, the rate of H_2 production reached a maximum at 20 μM [Ni^{2+}], whereas when the concentration of NC(520) was varied, the rate leveled off above 4.0 μM [NC] (Fig. S6). These results suggest that at [Ni^{2+}] of 20 μM or greater, the rate becomes limited by NC light absorption, whereas at [NC] of 4.0 μM, the system is limited by the H_2-forming reaction at Ni^{2+}. Similarly, the rate of H_2 production depends linearly on light intensity up to approximately 13 mW/cm^{-2} (Fig. S7). Overall, it appears that photon absorption by NCs and catalysis by Ni^{2+} have similar enough rates that each can be rate-limiting under different conditions.

Quantum yields for H_2 generation were determined for the system at [Ni^{2+}] = 20 μM (where the rate of H_2 evolution is controlled by [NC]) with NCs of different sizes. In water, the quantum yield ϕ based on two photons per H_2 evolved is 36 ± 10% at [NC(520)] = 1 to 2 μM, decreasing to 20 ± 2% at [NC(520)] = 4.0 μM (Supporting Online Material); similarly, $\phi(H_2)$ is 35 ± 4% at [NC(540)] = 4.0 μM. The quantum yield reaches 59 ± 8% when using a 1:1 EtOH/H_2O mixture as the solvent (Table S2). Complete conversion of all available light energy is presumably prevented by electron-hole recombination and/or fast non-radiative electronic relaxation.

We next sought to determine whether or not the active catalyst was on the NC surface or in solution during hydrogen photogeneration. After irradiation of a NC(540)-based H_2 generating system for 24 hours, the

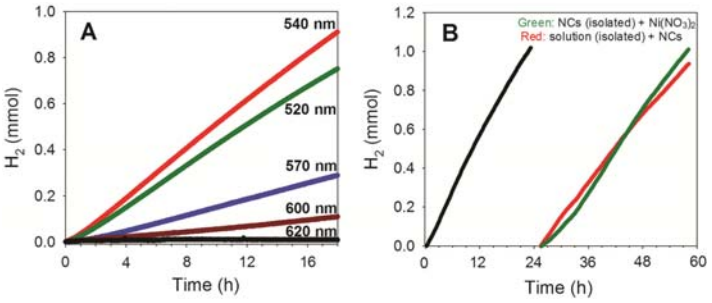

Fig. 3. (A) H_2 production from irradiation of aqueous solutions using different sizes of CdSe NCs (4.0 μM) labeled by the peak in their first excitonic absorption, 4.0 μM [$Ni(NO_3)_2$], and 0.5 M AA. **(B)** After 24 hours, an active solution was filtered to separate the NCs from the solution and the nickel(II) catalyst. After the separation, each individual component was inactive, but regained activity when the other was added.

NCs were separated from the solution by centrifugation and filtration, and each component was examined separately for its H_2 generating activity with added AA. Neither the NCs nor the solution was found to have any significant activity for photochemical H_2 generation. The chemical composition of the NCs and solution were each examined by atomic absorption spectroscopy, showing that > 97% of the Ni and < 3% of the Cd remained in solution while > 97% of Cd and < 3% of the Ni remained in the precipitated NCs (Table S3). Additionally, TEM (TEM) images of the separated NCs showed no significant change in NC size, and energy dispersive X-ray analysis showed no evidence of colloidal Ni deposited on the NC surface (Fig. S8-9). Addition of Ni^{2+} and AA to the NCs restored activity for H_2 production upon resuspension; likewise, when fresh NC(540) and AA were added to the Ni-containing solution, we observed activities that were similar to those during the initial irradiation (Fig. 3B). The results indicate that the active catalyst is a Ni species generated in solution, and that the NCs maintain their ability to act as the photosensitizer during the catalytic process.

The use of different Ni^{2+} salts ($Ni(NO_3)_2$, $NiCl_2$ and $Ni(acetate)_2$) produced a similar level of H_2 production activity, suggesting that the actual catalyst is generated in situ. Because DHLA binds to Ni^{2+} with binding constants near or above 10^{10} (*24*), and nickel-thiolates have previously been reported as catalysts for light-driven hydrogen production (*25*), we focused on DHLA as a potential chelating ligand toward nickel. Maintaining a solution of NC(520) at pH 4.5 under N_2 in the absence of light for 5 hours and centrifuging to precipitate the NCs gave a solution with 8 to 14 molecules of DHLA per NC, which had apparently dissociated from the NC. Thus the formation of a Ni^{2+}-DHLA complex is both possible and favorable in the catalytic solutions. Adding up to 100 equivalents of excess DHLA gave similar activity toward H_2 production (Fig. S10), but addition of EDTA (which sequesters Ni^{2+} and prevents formation of a Ni^{2+}-DHLA complex) eliminated activity (Fig. S11). Addition of colloidal Ni^0 (4 nm in diameter) in place of the nickel(II) salt gave no significant amount of H_2 under the standard catalytic conditions (Fig. S11). Synthesizing the Ni^{2+}-DHLA catalyst *ex situ* and adding it to the NC solution (in place of Ni^{2+} salts) gives the same overall activity for H_2 production. Altogether, these experiments are consistent with a soluble nickel(II)-DHLA species being catalytically active. Finally, electrochemical studies on independently prepared 1:1 Ni^{2+}-DHLA solutions (0.2 μM in 1:1 EtOH/H2O) showed a cathodic feature at -0.9 V vs. NHE that appears only upon addition of acid (Fig. S12), indicating that Ni-DHLA can reduce protons catalytically, and at a potential comparable to that produced by the excited NCs.

Although we have not yet determined the structure of the catalytically active nickel species, spectroscopic studies on Ni^{2+}-DHLA help to understand the predominant forms of nickel in solution. The UV-visible spectrum of a 1:5 mixture of Ni^{2+} (50 μM) and DHLA (250 μM) at pH 4.5 is very similar to that generated with a mixture of Ni^{2+} (50 μM) and 1,3-propanedithiol, suggesting that Ni^{2+} coordinates via the S donors of DHLA (Fig. S13). The absorption maxima from a 1:1 Ni-DHLA solution follow Beer's Law between 5.0 and 500 μM, suggesting that nickel speciation does not change over the [Ni^{2+}] and [DHLA] concentrations employed in the catalytic experiments (Fig. S14). A Job plot of Ni^{2+} and DHLA in this concentration regime has a maximum at a metal/DHLA ratio of roughly 1:1, suggesting that the predominant complex has one DHLA per Ni^{2+} (Fig. S14). X-ray crystal structures of nickel complexes with related dithiols (including 1,3-propanedithiol) have shown multimetallic structures containing square-planar nickel(II) centers bridged by thiolates, with stoichiometries such as 3:4, 4:4, 6:6, and 6:7 (*26–28*). Because nickel-thiolate species are labile in solution, many nickel species are accessible under the reaction conditions, and detailed mechanistic studies will be necessary to identify the one(s) responsible for proton reduction in this system.

A light-driven system for the photogeneration of hydrogen that consists of simple components containing only Earth-abundant elements could have a significant impact on the sustainable production of chemical fuels. Further, the robustness of the system may be generalizable to other nanoparticle systems, such as Type II NCs and dot-in-rod NCs (*6*, *10*), which are better engineered for charge separation. When considering the efficiency of this system in a real-world context, further improvements could be made by adding light-harvesting components that absorb more of the solar spectrum, since with NC(540) only about 25% of the available solar flux is absorbed. Nonetheless, this particular NC-DHLA-Ni system exhibits high activity for proton reduction and impressive durability, which suggests that it could also serve as a valuable component in complete artificial photosynthetic water splitting systems for light-to-chemical energy conversion.

References and Notes

1. N. S. Lewis, D. G. Nocera, Powering the planet: chemical challenges in solar energy utilization. *Proc. Natl. Acad. Sci. U.S.A.* **103**, 15729 (2006). doi:10.1073/pnas.0603395103 Medline
2. J. H. Alstrum-Acevedo, M. K. Brennaman, T. J. Meyer, Chemical approaches to artificial photosynthesis. 2. *Inorg. Chem.* **44**, 6802 (2005). doi:10.1021/ic050904r Medline
3. A. J. Bard, M. A. Fox, Artificial Photosynthesis: Solar Splitting of Water to Hydrogen and Oxygen. *Acc. Chem. Res.* **28**, 141 (1995). doi:10.1021/ar00051a007
4. A. J. Esswein, D. G. Nocera, Hydrogen production by molecular photocatalysis. *Chem. Rev.* **107**, 4022 (2007). doi:10.1021/cr050193e Medline
5. W. T. Eckenhoff, R. Eisenberg, Molecular systems for light driven hydrogen production. *Dalton Trans.* **41**, 13004 (2012). doi:10.1039/c2dt30823a Medline
6. L. Amirav, A. P. Alivisatos, Photocatalytic Hydrogen Production with Tunable Nanorod Heterostructures. *J. Phys. Chem. Lett.* **1**, 1051 (2010). doi:10.1021/jz100075c
7. K. A. Brown, S. Dayal, X. Ai, G. Rumbles, P. W. King, Controlled assembly of hydrogenase-CdTe nanocrystal hybrids for solar hydrogen production. *J. Am. Chem. Soc.* **132**, 9672 (2010). doi:10.1021/ja101031r Medline
8. Y. Shemesh, J. E. Macdonald, G. Menagen, U. Banin, Synthesis and Photocatalytic Properties of a Family of CdS-PdX Hybrid Nanoparticles. *Angew. Chem. Int. Ed.* **50**, 1185 (2011). doi:10.1002/anie.201006407
9. K. A. Brown, M. B. Wilker, M. Boehm, G. Dukovic, P. W. King, Characterization of photochemical processes for H2 production by CdS nanorod-[FeFe] hydrogenase complexes. *J. Am. Chem. Soc.* **134**, 5627 (2012). doi:10.1021/ja2116348 Medline
10. H. Zhu, N. Song, H. Lv, C. L. Hill, T. Lian, Near unity quantum yield of light-driven redox mediator reduction and efficient H2 generation using colloidal nanorod heterostructures. *J. Am. Chem. Soc.* **134**, 11701 (2012). doi:10.1021/ja303698e Medline
11. F. Wang *et al.*, A Highly Efficient Photocatalytic System for Hydrogen Production by a Robust Hydrogenase Mimic in an Aqueous Solution. *Angew. Chem. Int. Ed.* **50**, 3193 (2011). doi:10.1002/anie.201006352
12. M. A. Holmes, T. K. Townsend, F. E. Osterloh, Quantum confinement controlled photocatalytic water splitting by suspended CdSe nanocrystals. *Chem. Commun. (Camb.)* **48**, 371 (2012). doi:10.1039/c1cc16082f Medline
13. D. V. Talapin *et al.*, CdSe/CdS/ZnS and CdSe/ZnSe/ZnS Core−Shell−Shell Nanocrystals. *J. Phys. Chem. B* **108**, 18826 (2004). doi:10.1021/jp046481g
14. Materials and Methods are available in the online Supplementary Materials.
15. G. M. Brown, B. S. Brunschwig, C. Creutz, J. F. Endicott, N. Sutin, Homogeneous catalysis of the photoreduction of water by visible light. Mediation by a tris(2,2′-bipyridine)ruthenium(II)-cobalt(II) macrocycle system. *J. Am. Chem. Soc.* **101**, 1298 (1979). doi:10.1021/ja00499a051
16. B. Probst, M. Guttentag, A. Rodenberg, P. Hamm, R. Alberto, Photocatalytic H2 production from water with rhenium and cobalt complexes. *Inorg. Chem.* **50**, 3404 (2011). doi:10.1021/ic102317u Medline
17. B. F. DiSalle, S. Bernhard, Orchestrated photocatalytic water reduction using surface-adsorbing iridium photosensitizers. *J. Am. Chem. Soc.* **133**, 11819 (2011). doi:10.1021/ja201514e Medline
18. T. M. McCormick *et al.*, Reductive side of water splitting in artificial photosynthesis: new homogeneous photosystems of great activity and mechanistic insight. *J. Am. Chem. Soc.* **132**, 15480 (2010). doi:10.1021/ja1057357 Medline

19. W. R. McNamara *et al*., Cobalt-dithiolene complexes for the photocatalytic and electrocatalytic reduction of protons in aqueous solutions. *Proc. Natl. Acad. Sci. U.S.A.* **109**, 15594 (2012). doi:10.1073/pnas.1120757109 Medline
20. A. Fihri *et al*., Cobaloxime-Based Photocatalytic Devices for Hydrogen Production. *Angew. Chem. Int. Ed.* **47**, 564 (2008). doi:10.1002/anie.200702953
21. D. Streich *et al*., High-turnover photochemical hydrogen production catalyzed by a model complex of the [FeFe]-hydrogenase active site. *Chemistry* **16**, 60 (2010). doi:10.1002/chem.200902489 Medline
22. T. A. White, B. N. Whitaker, K. J. Brewer, Discovering the balance of steric and electronic factors needed to provide a new structural motif for photocatalytic hydrogen production from water. *J. Am. Chem. Soc.* **133**, 15332 (2011). doi:10.1021/ja206782k Medline
23. J. Jasieniak, M. Califano, S. E. Watkins, Size-dependent valence and conduction band-edge energies of semiconductor nanocrystals. *ACS Nano* **5**, 5888 (2011). doi:10.1021/nn201681s Medline
24. F. Bonomi *et al*., Synthesis and characterization of metal derivatives of dihydrolipoic acid and dihydrolipoamide. *Inorg. Chim. Acta* **192**, 237 (1992). doi:10.1016/S0020-1693(00)80765-3
25. Z. Han, W. R. McNamara, M. S. Eum, P. L. Holland, R. Eisenberg, A Nickel Thiolate Catalyst for the Long-Lived Photocatalytic Production of Hydrogen in a Noble-Metal-Free System. *Angew. Chem. Int. Ed.* **51**, 1667 (2012). doi:10.1002/anie.201107329
26. M. Kockerling, G. Henkel, Synthesis and structure of [Ni4(S2C7H10)4], the first tetranuclear cyclic nickel complex with bifunctional thiolate ligands and of the mononuclear precursor compound Na2[Ni(S2C7H10)2]·4MeOH·iPrOH. *Inorg. Chem. Commun.* **3**, 117 (2000). doi:10.1016/S1387-7003(00)00027-7
27. J. Sletten *et al*., The structure of a toroidal, neutral, homoleptic Ni(II) complex with a chelate dithiolate ligand, [Ni6(SCH2CH2CH2S)6]. *Acta Chem. Scand.* **48**, 929 (1994). doi:10.3891/acta.chem.scand.48-0929 Medline
28. W. Tremel, M. Kriege, B. Krebs, G. Henkel, Nickel-thiolate chemistry based on chelating ligands: controlling the course of self-assembly reactions via ligand bite distances. Synthesis, structures, and properties of the homoleptic complexes [Ni3(SCH2C6H4CH2S)4]2-, [Ni3(SCH2CH2S)4]2-, and [Ni6(SCH2CH2CH2S)7]2-. *Inorg. Chem.* **27**, 3886 (1988). doi:10.1021/ic00295a004
29. D. H. Chen, S. H. Wu, Synthesis of Nickel Nanoparticles in Water-in-Oil Microemulsions. *Chem. Mater.* **12**, 1354 (2000). doi:10.1021/cm991167y
30. I. C. Gunsalus, L. S. Barton, W. Gruber, *J. Am. Chem. Soc.* **78**, 1763 (1956). doi:10.1021/ja01589a079
31. J. Aldana, N. Lavelle, Y. Wang, X. Peng, Size-dependent dissociation pH of thiolate ligands from cadmium chalcogenide nanocrystals. *J. Am. Chem. Soc.* **127**, 2496 (2005). doi:10.1021/ja047000+ Medline
32. J. W. Kung *et al*., Reversible biological Birch reduction at an extremely low redox potential. *J. Am. Chem. Soc.* **132**, 9850 (2010). doi:10.1021/ja103448u Medline
33. K. A. Connors, Binding Constants: The Measurement of Molecular Complex Stability (Wiley-Interscience Press, 1987).
34. B. M. Tolbert, J. B. Ward, Dehydroascorbic acid. In *Ascorbic Acid: Chemistry, Metabolism, and Uses*; P. A. Seib, B. M. Tolbert, Eds.; (Advances in Chemistry Series 200; American Chemical Society: Washington, DC, 1982).
35. J. Hvoslef *et al*., The Structure of Dehydroascorbic Acid in Solution. *Acta Chem. Scand. B* **33**, 503 (1979). doi:10.3891/acta.chem.scand.33b-0503
36. S. Berger, Vitamin C—A 13C magnetic resonance study. *Tetrahedron* **33**, 1587 (1977). doi:10.1016/0040-4020(77)80166-X

Acknowledgments: ZH led the effort for hydrogen generation and catalysis, and FQ for nanocrystal synthesis and characterization. This work was supported by the Office of Basic Energy Sciences, U. S. Department of Energy, Grant DE-FG02-09ER16121. The authors acknowledge the University of Rochester Medical Center and the Department of Environmental Medicine for the analytical support of Robert M. Gelein for the cadmium and nickel measurements.

Supplementary Materials

www.sciencemag.org/cgi/content/full/science.1227775/DC1
Materials and Methods
Figs. S1 to S16
Tables S1 to S3
References (*29*–*36*)
10.1126/science.1227775

23 July 2012; accepted 10 October 2012
Published online 08 November 2012